

Figure 2.6. Interconversion of (a) a 9×250 mm column packed with unfunctionalized AS1 PS-DVB co-polymer between 2 mM benzoic acid and water forms (reproduced with permission from Ref. 34) and (b) a 4×250 mm Dionex IonPac NS1 reversed-phase ethylvinylbenzene-divinylbenzene polymer between 2 mM benzoic acid and water forms. The flow-rate was 1 mL/min, detector UV/Vis (210 nm) and the temperature was 30°C in each case.

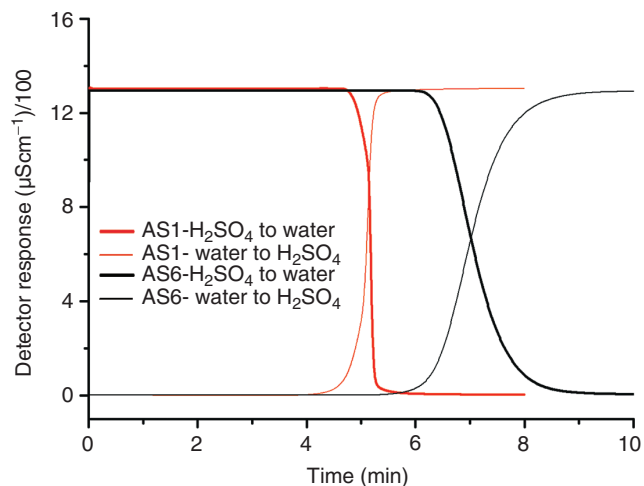


Figure 2.9. Column conversion from water to 2 mM H_2SO_4 form and vice versa. IonPac ICE-AS1 and IonPac ICE-AS6 stationary phases were tested. Experimental conditions: analytical system DX500, eluent flow-rate 1 mL/min, column temperature was 30°C .

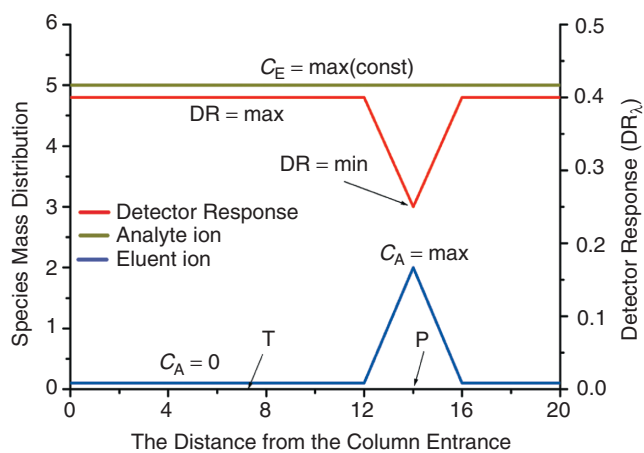


Figure 2.11. Schematic diagram of indirect UV/Vis detection in IEC. The analyte and eluent mass-distribution is shown on the left y -axis and the corresponding UV/Vis absorbance is shown on the right y -axis. The eluent concentration is not affected by the presence of the analyte peak due to nonactive eluent participation in the IEC separation mechanism.

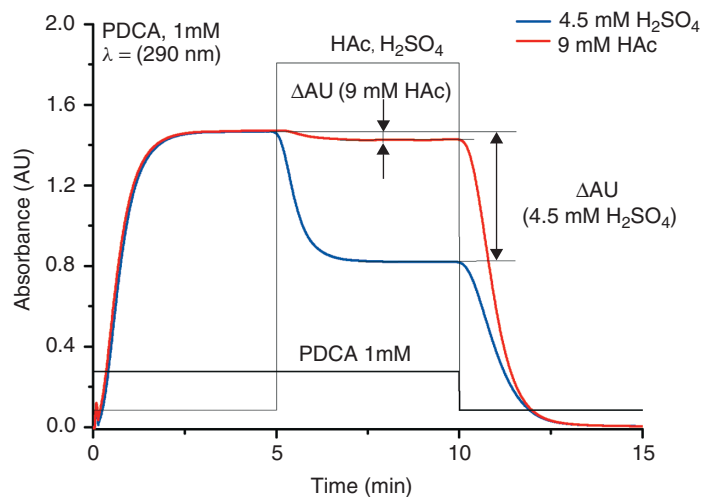


Figure 2.13. Absorbance measurements of 1 mM PDCA injected with a plug of 9 mM H_2SO_4 (dark gray line) or 9 mM acetic acid (HAc, dark gray line) in a continuous flow analyzer. The total flow-rate through the detector was 1.0 mL/min, absorbance was measured at 290 nm. The PDCA gradient is marked by thicker gray line, while sulfuric or acetic acids gradients are marked by thinner gray lines.

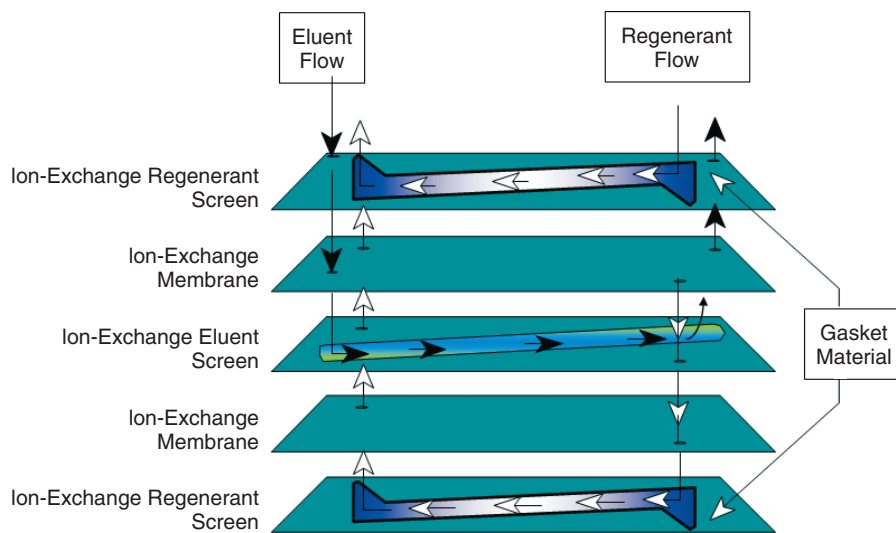


Figure 4.1. A flat membrane based suppressor design schematic.

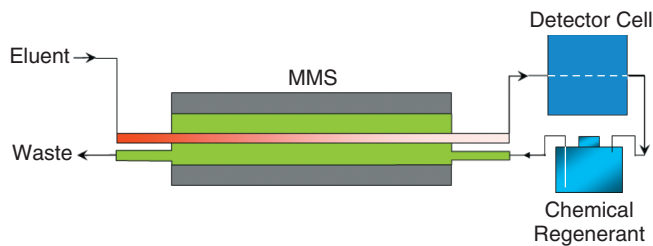


Figure 4.2. DCR setup with a Micromembrane suppressor and detector cell.

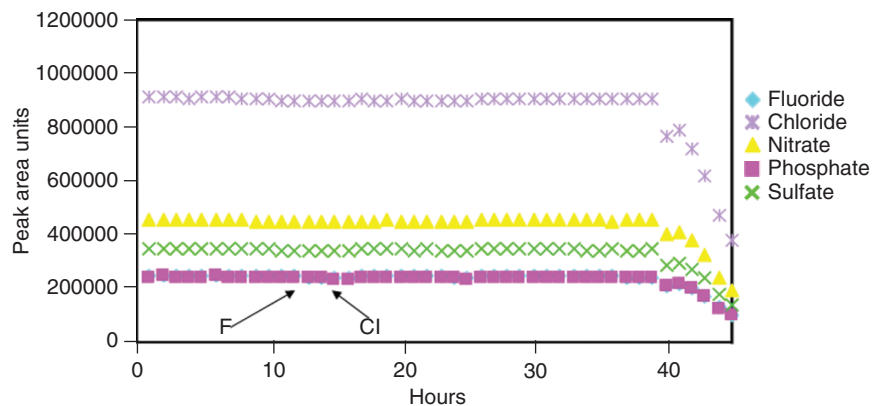


Figure 4.3. Peak area response versus time (hours) for a DCR setup where the 2L regenerant reservoir is actively mixed using a stirrer. Column: IonPac® AS15 (4 × 250 mm); Eluent: NaOH 38 mM at 1.2 mL/min; Regenerant: 75 mN Sulfuric acid. Standards: A 10x dilution of a 5 anion standard. (Dionex Corporation P/N 037157).

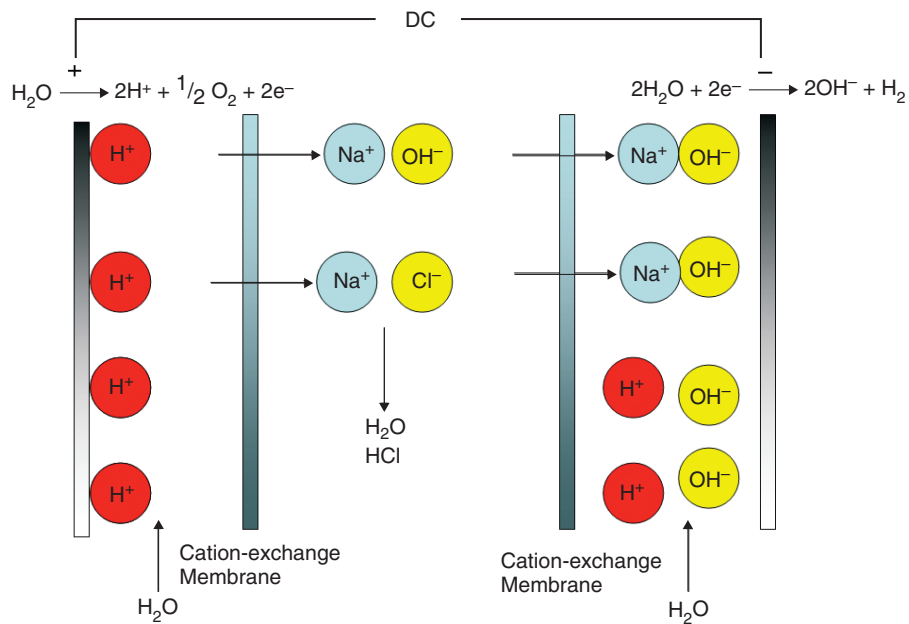


Figure 4.4. SRS suppressor operational schematic.

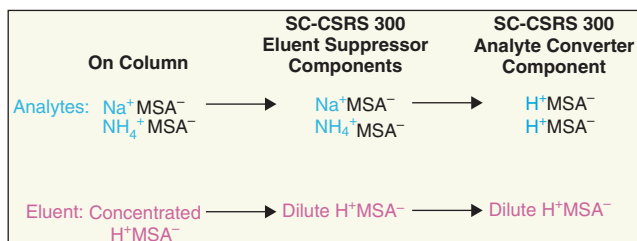


Figure 4.5. Salt converter net reaction schematic.

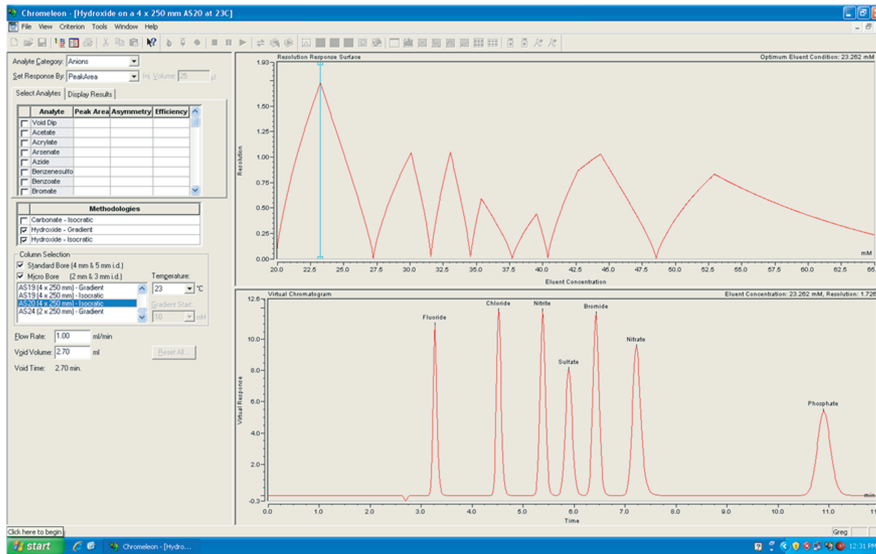


Figure 5.2. Virtual Column interface for the isocratic separation of inorganic anions using a Dionex IonPac AS20 column.

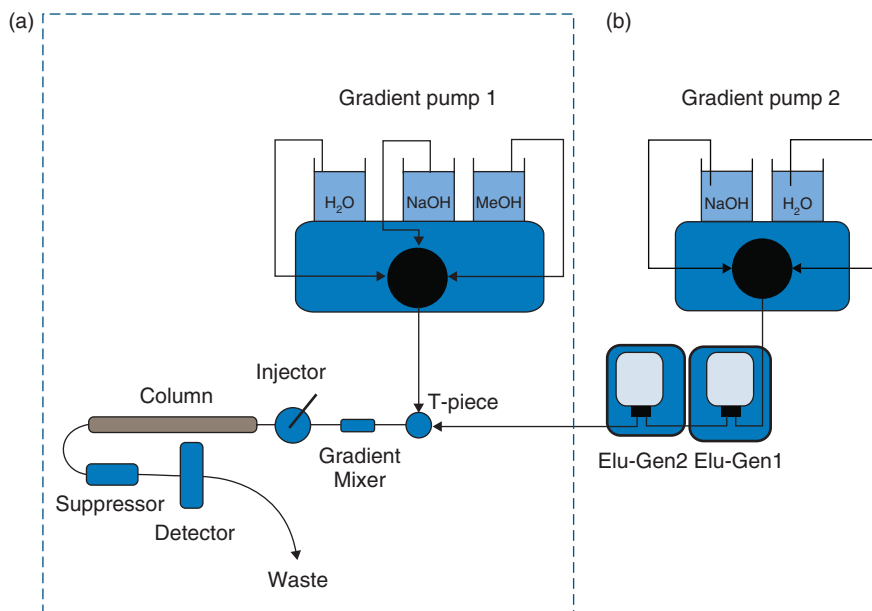


Figure 5.4. Schematic of pump layout used by Zakaria et al. to facilitate use of methanol with non compatible IC components. Layout (a) avoids methanol compatibility issues by removing the Elu-Gen modules and using a manually prepared hydroxide stock solution. Layout (b) avoids passing methanol through the Elu-Gen modules by mixing it with the eluent stream subsequent to hydroxide generation. (Taken from 14.)

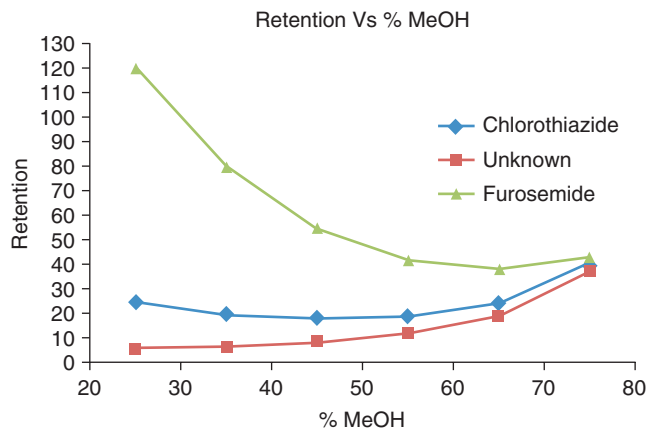


Figure 5.7. Retention vs. %MeOH for three of the test compounds investigated. (Taken from 24.)

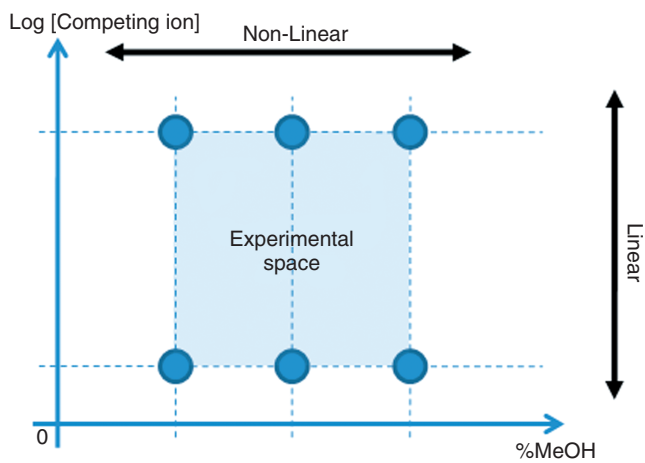


Figure 5.8. Experimental space used by Zakaria et al. for two-dimensional IC modeling. The two variables used are competing ion and methanol concentrations.

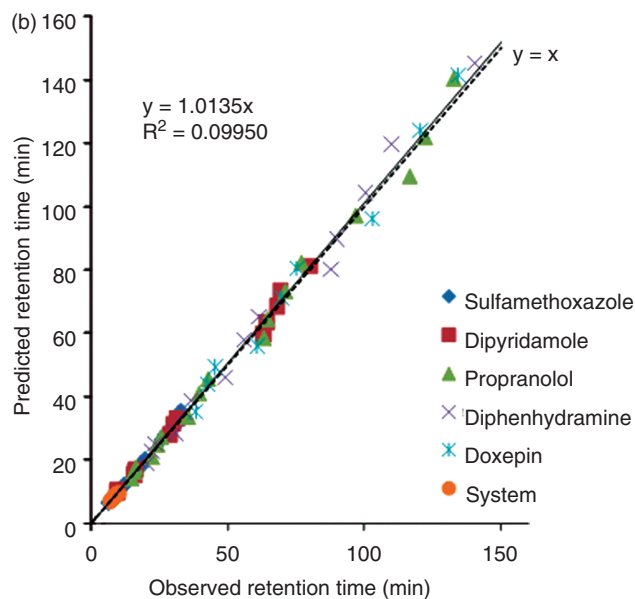
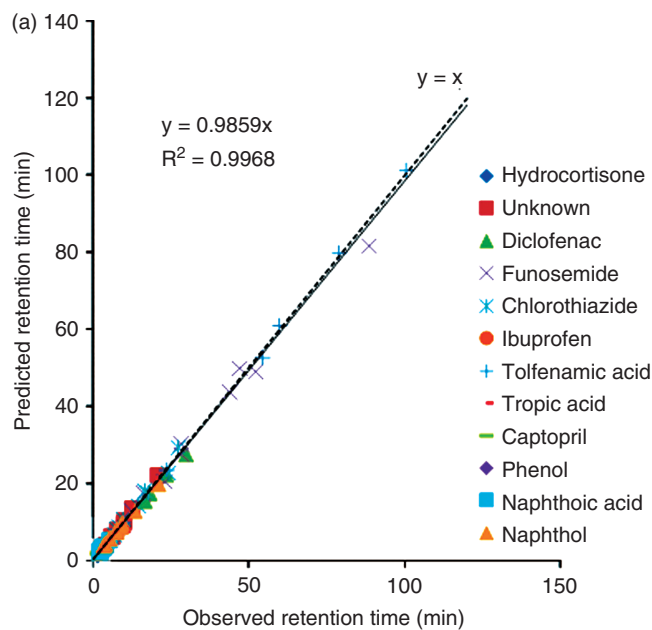


Figure 5.9. Observed and predicted retention times for anions (a) and cations (b) using the two-dimensional model of Zakaria et al. The solid line represents the line of best fit through the predicted vs. observed data while the dotted line represents $y = x$, i.e. perfect agreement between observed and predicted values. (Taken from 24.)

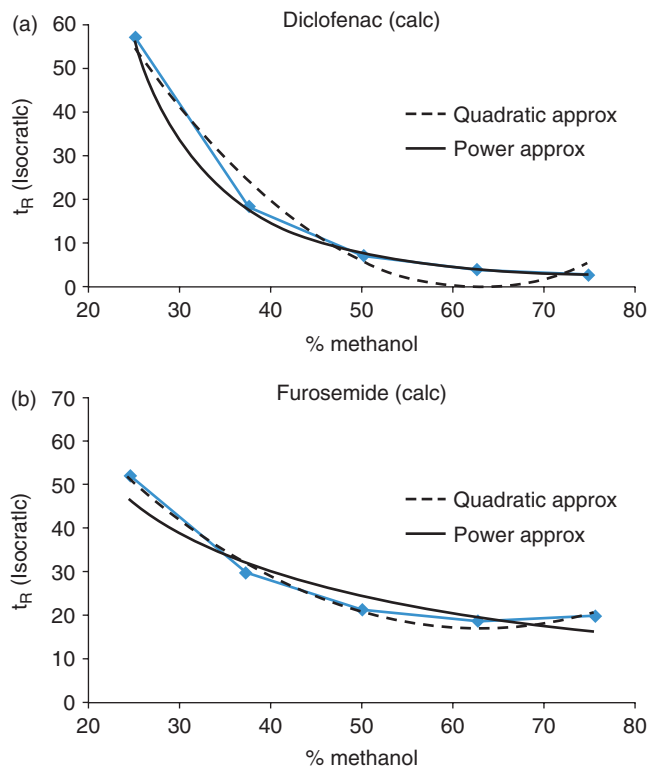


Figure 5.10. Comparison of curve approximations used to describe t_R vs. MeOH plots. (Taken from 24.)

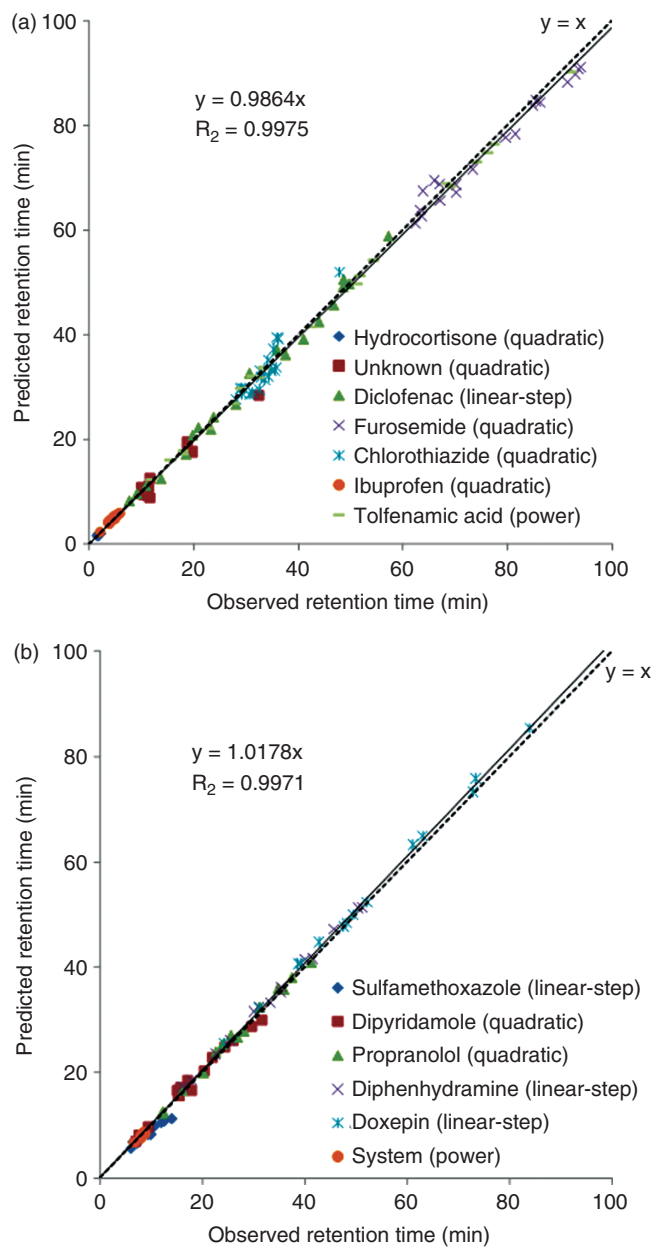


Figure 5.11. Correlation between observed and predicted retention times. (a) Pharmaceutical anions using 20 multi step conditions comprising 2 and 3-step methanol gradient profiles at 30 mM hydroxide. (b) Pharmaceutical cations using 14 multi step conditions comprising 2 and 3-step methanol gradient profiles at 20 mM MSA. The solid and dotted lines have the same meaning as in Figure 5.9. (Taken from 24.)

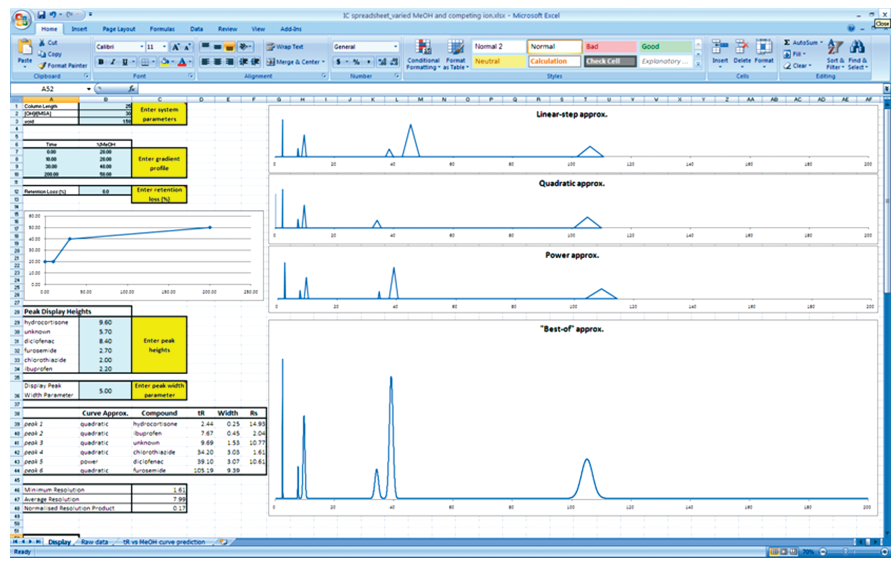


Figure 5.12. Methanol gradient and two-dimensional isocratic spreadsheet of Zakaria et al. 24.

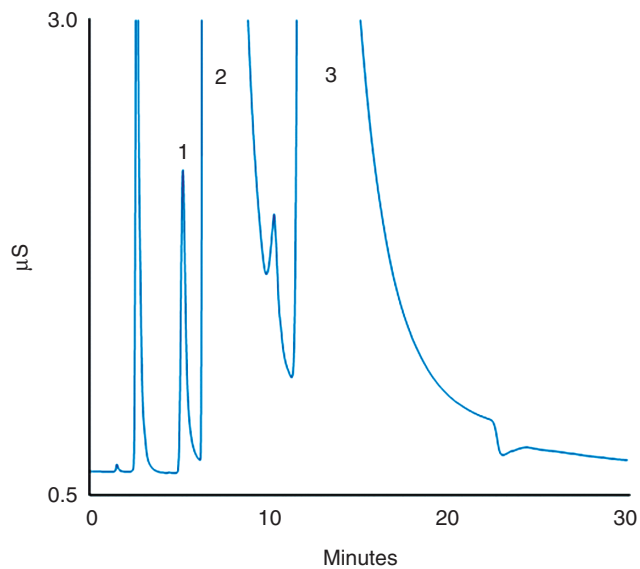


Figure 7.2. Determination of NMP in a simulated Cefepime for Injection. Ion chromatographic conditions: column, IonPac[®] CG17 guard and CS17 analytical; eluent, 6 mM MSA from 0 to 7.5 min, 85 mM from 7.5 to 20 min, and 6 mM from 20 to 30 min, 0.4 mL/min; column temperature, 40° C; injection volume, 5 µL; suppressed conductivity detection. Sample: 10 mg/mL cefepime hydrochloride + 7.25 mg/mL arginine. Peaks: 1, NMP (0.25%); 2, arginine; and 3, cefepime. [Chromatogram obtained from Dionex Corporation with permission].

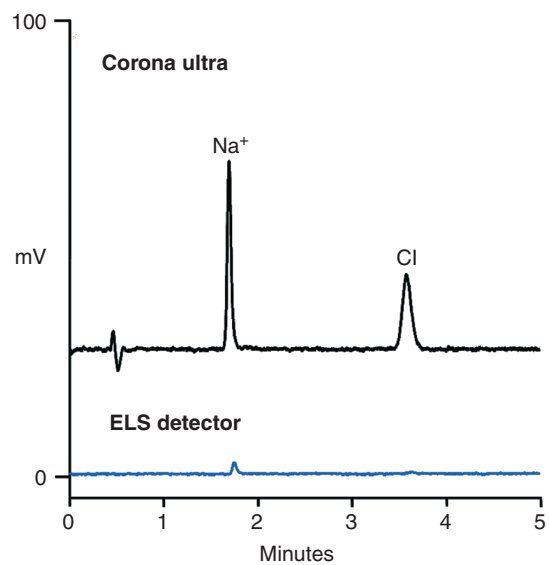


Figure 10.1. Separation of sodium and chloride (5 ng on column) using an Acclaim Trinity P1 $3\ \mu\text{m}\ 3.0 \times 50\ \text{mm}$ column with flow at 0.6 mL/min. Analytes were measured using either a charged aerosol detector (Corona *ultra*) or ELSD (Sedex-85). Mobile phase: 60/40 v/v acetonitrile /15 mM ammonium acetate buffer, pH = 5.2. Corona *ultra* settings: Nebulizer T – 35°C, Range – 100 pA full scale, Filter - Off. Sedex-85 settings: Evaporation T – 45°C; Gain - 10; Filter - Off.

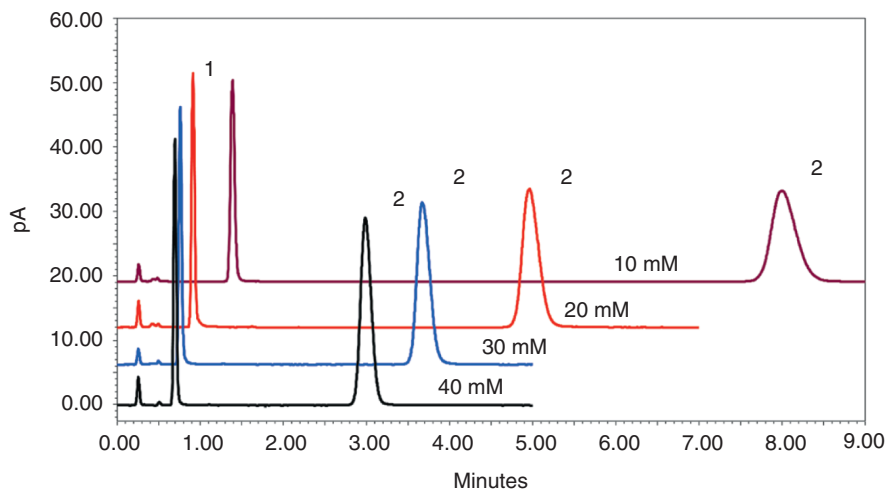


Figure 10.5. Overlay of chromatograms of diclofenac sodium salt (~500 ng on column) separated using an Acclaim Trinity P1, 3 μm 3.0 \times 50 mm at 1.0 mL/min. Mobile phase 75/25 v/v acetonitrile/ ammonium acetate pH = 4.8, buffer strength adjusted to 10, 20, 30, and 40 mM total buffer strength. Detector settings Corona *ultra*; Filter = med; Neb Temp = 25°C. Peak Identification; 1. sodium, 2. diclofenac.

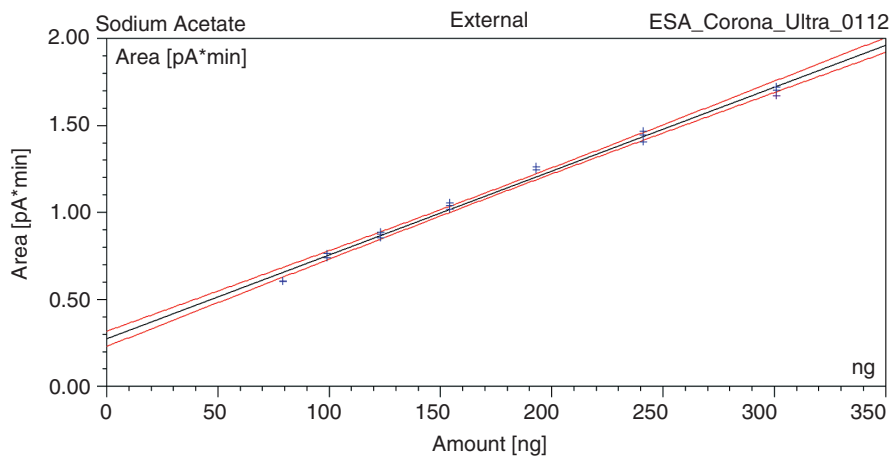


Figure 10.6. Sodium acetate from 80 to 300 ng on column (7 points with 3 injections at each point), fit with linear regression ($R^2 = 0.994$). Upper and lower 95% confidence limits are displayed.

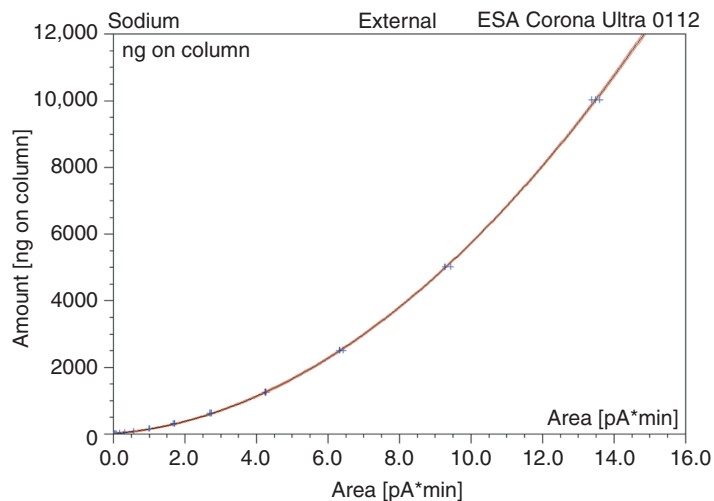


Figure 10.7. Sodium acetate from 5 ng to 10 μg on column (12 points with three injections at each point) fit with a polynomial and inverted X and Y axis ($R^2 = 0.9997$). Upper and lower 95% confidence limits are displayed.

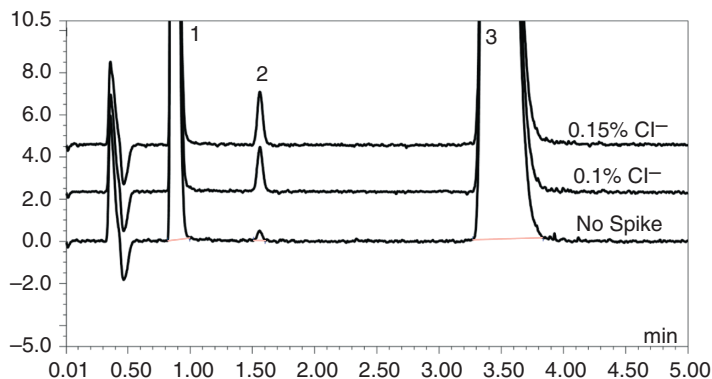


Figure 10.8. Overlay of chromatograms of diclofenac sodium salt samples (5.7 μg on column) with 0, 0.1% and 0.15% (w/w) chloride spikes. Conditions: Dionex Acclaim Trinity P1, 3 μm 3.0 \times 50 mm flow at 0.8 mL/min. Mobile phase 75/25 v/v acetonitrile/120 mM ammonium acetate pH = 4.8. Detector settings: Corona *ultra*; Filter = med; Neb Temp = 25°C. Peak Identification; 1. sodium, 2. chloride, 3. diclofenac.

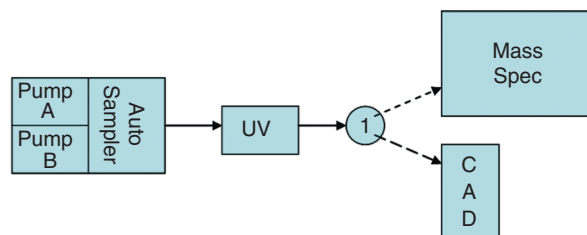


Figure 10.9. A schematic of the multi-detector platform. An adjustable flow splitter (1) was set to deliver 80 $\mu\text{L}/\text{min}$ to the single-quad MS and 0.42 mL/min to the Corona CAD when using a flow-rate of 0.5 mL/min total flow.

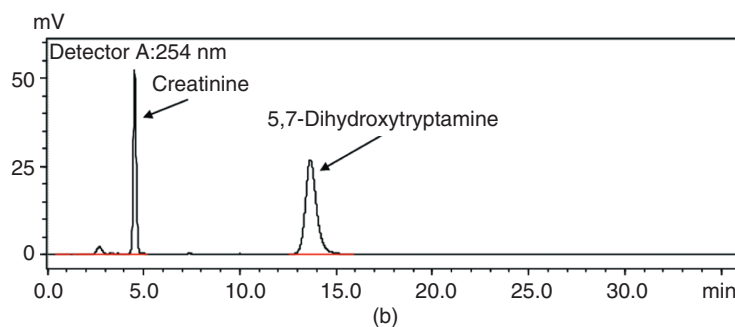
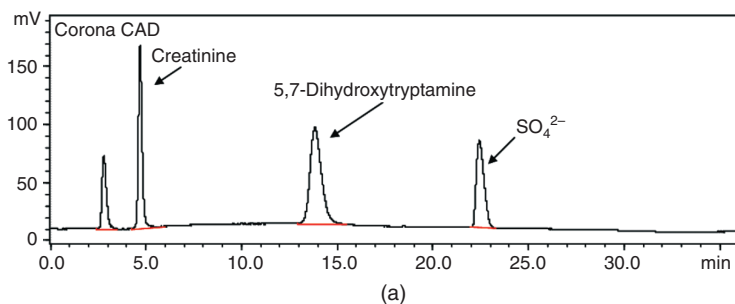


Figure 10.10. Separation of DHT creatinine sulfate ($\sim 2 \mu\text{g}$ on column) on a Sequant ZIC[®]-pHILIC, 5- μm 4.6 \times 150 mm column at 30°C using a binary gradient flow at 0.5 mL/min. Mobile Phase A: 15/5/20/60 (v/v), 100 mM ammonium acetate (pH 4.6)/methanol/isopropyl alcohol/acetonitrile; Mobile Phase B: 50/5/20/25 (v/v) 30 mM ammonium acetate pH 4.6/methanol/isopropyl alcohol/acetonitrile. Gradient (time min., %B): 0, 20; 3, 20; 24, 70; 26, 70; 32, 15; 33, 20; 36, 20. (a) Corona CAD detection: 100 pA full scale; filter—none. (b) UV/Vis detection at 254 nm. (d) Mass spectrum for creatinine (MW = 113.1) at retention time 5.7 minutes. (e) Mass spectrum for DHT (MW = 192.2) retention time 5.7 minutes. LC-ESI-MS: Acquisition Mode, Scan; Polarity, Positive; Event Time, 1.00 sec; Detector Voltage, 1.5 kV; Start m/z = 100; End m/z = 500; Scan speed, 500.

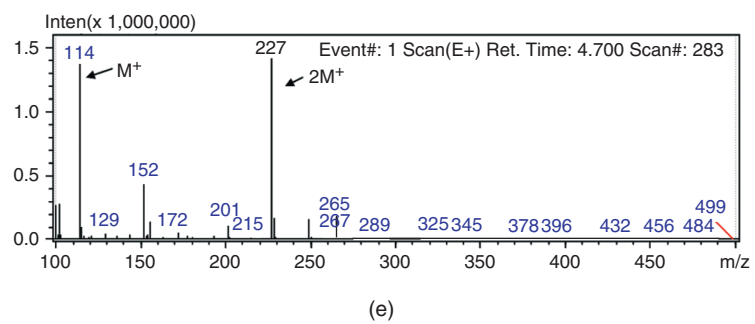
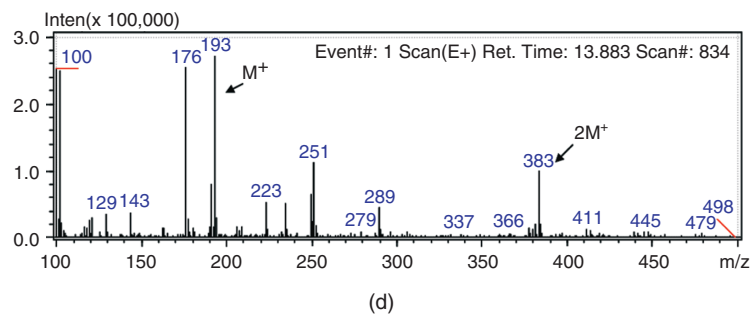


Figure 10.10. (Continued)

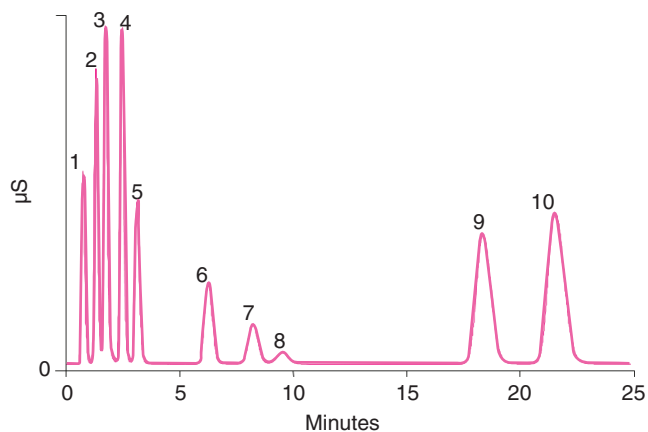


Figure 11.3. Separation of Group I and Group II cations from carbachol and choline. The analytes are separated on an IonPac CS17 (4 × 250 mm) column with IonPac CG17 guard (4 × 50 mm) with a 5 mM methanesulfonic acid eluent produced by an eluent generator and flowing at 1.0 mL/min. The column temperature is 30°C and the injection volume 25 µL. The analytes are detected by suppressed conductivity detection using a CSRS-ULTRA II suppressor. The peak identities with concentrations in mg/L are: 1-lithium, 0.1; 2-sodium, 0.4; 3-ammonium, 0.5; 4-potassium, 1.0; 5-dimethylamine, 1.0; 6-choline, 1.0; 7-carbachol, 1.0; 8-bethanechol, 1.0; 9-magnesium, 0.5; 10-calcium, 1.0.

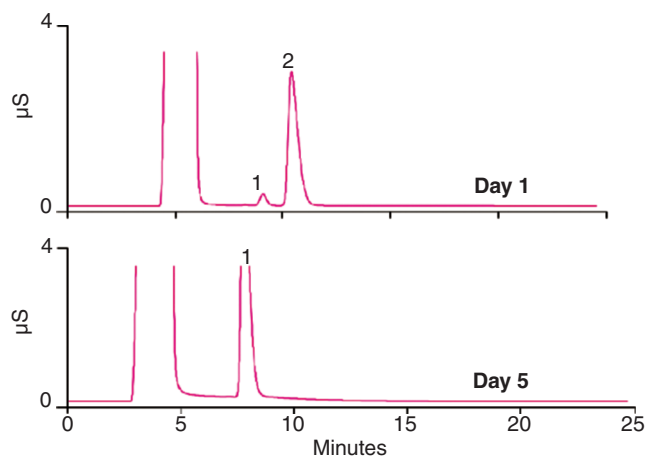


Figure 11.4. Base-catalyzed decomposition of carbachol to choline. Peak 1 is choline and peak 2 is carbachol. The concentrations of choline on days 1 and 5 are 42.2 and 502 mg/L, respectively and the concentration of carbachol on day one is 502 mg/L. The chromatography conditions are the same as Figure 11.3.

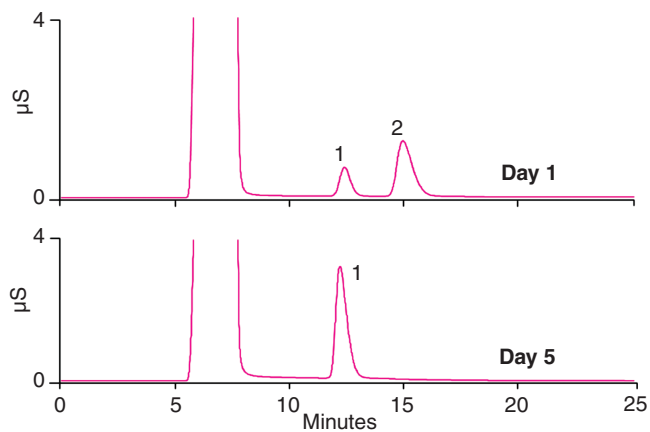


Figure 11.5. Conversion of bethanechol to 2-HPTA in alkaline solution. Peak 1 is 2-HPTA and peak 2 is bethanechol. The concentrations of 2-HPTA on days 1 and 5 are 101 and 501 mg/L, respectively, and the concentration of bethanechol on day one is 401 mg/L. The chromatography conditions are the same as Figure 11.3.

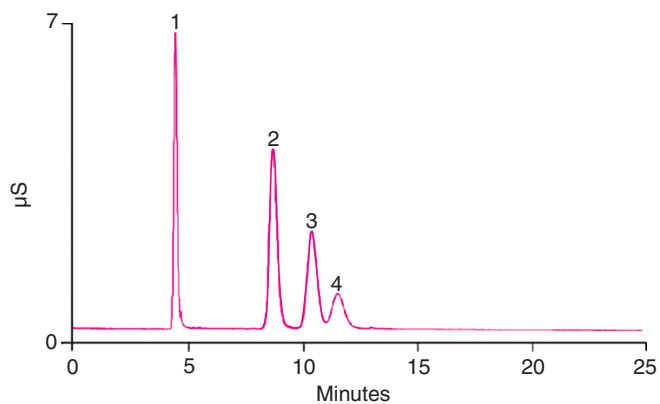


Figure 11.6. Determination of choline, carbachol, and bethanechol in lens and saline solutions. The peak identities with concentrations in mg/L are: 1- sodium, 0.031; 2-choline, 0.987; 3-carbachol, 0.967; 4- bethanechol, 0.985. The chromatography conditions are the same as Figure 11.3.

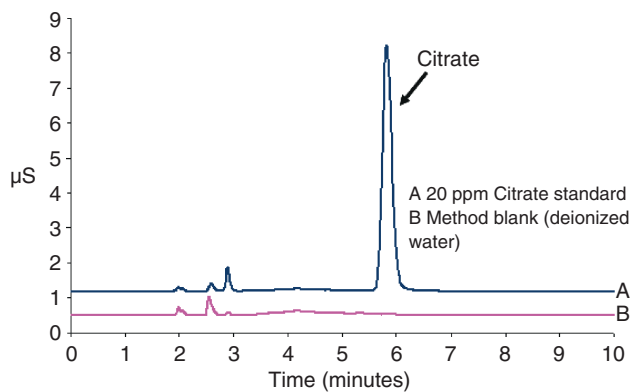


Figure 12.1. Chromatogram of 20 mg/L citrate standard and deionized water blank.

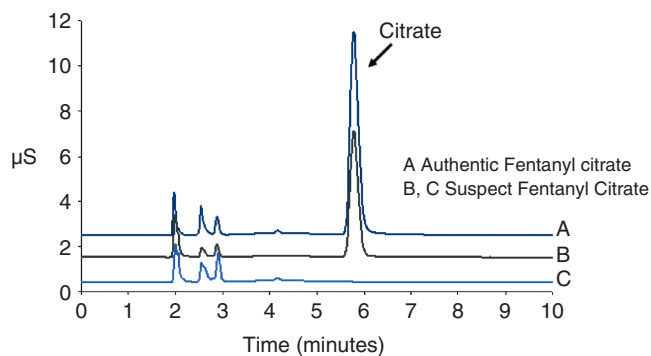


Figure 12.2. Chromatogram of authentic and suspect fentanyl citrate injectables.

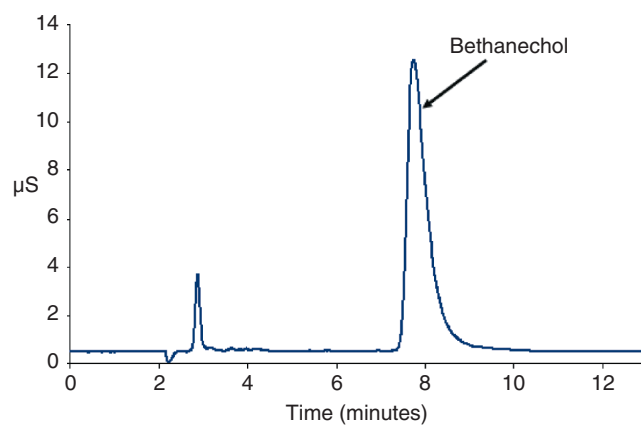


Figure 12.5. Bethanechol chloride standard in distilled deionized water (0.11 mg/mL).

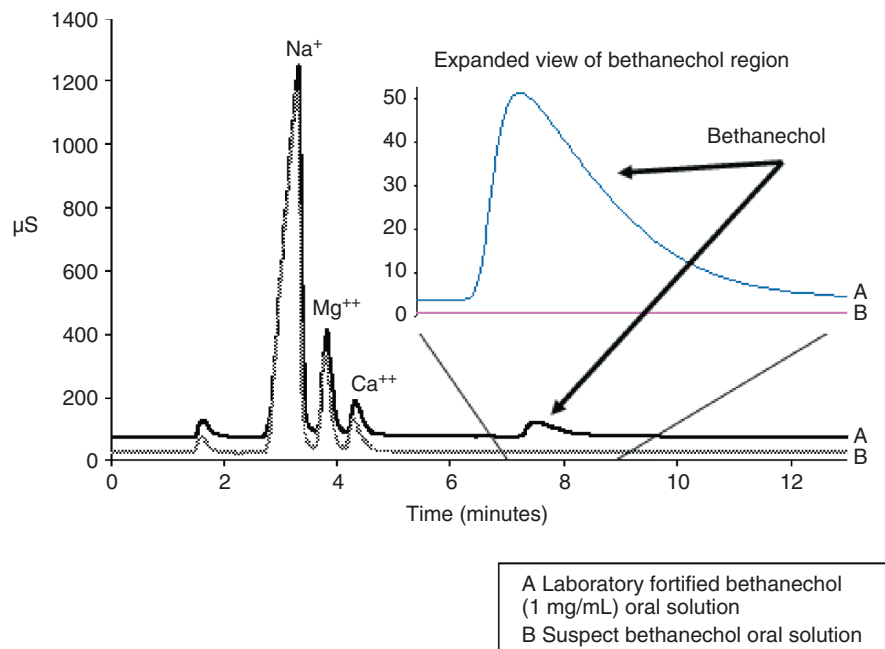


Figure 12.6. Chromatogram of suspect and laboratory fortified bethanechol oral solutions.

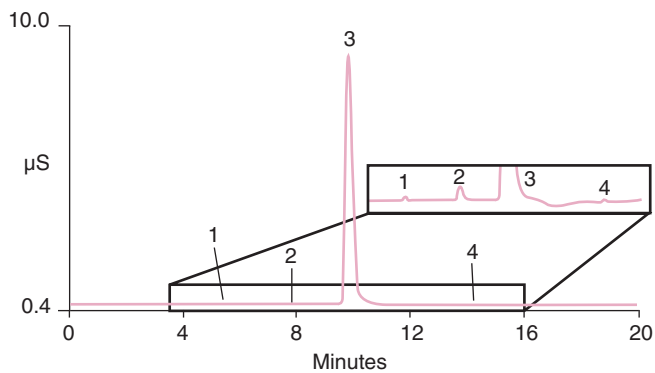


Figure 13.2. Separation of sulfate and anionic impurities in USP-grade paromomycin sulfate. Column: IonPac AS18 (2 × 250 mm); eluent: 22 mM KOH 0–7 min, then 22–40 mM 7–8 min, then 40 mM 8–20 min; eluent source: eluent generator cartridge; flow rate: 0.25 mL/min; column temperature: 30°C; detection: suppressed conductivity; injection volume: 5 µL; analyte concentrations: (1) 0.016% chloride, (2) carbonate, (3) 23.6% sulfate, (4) 0.040% phosphate.

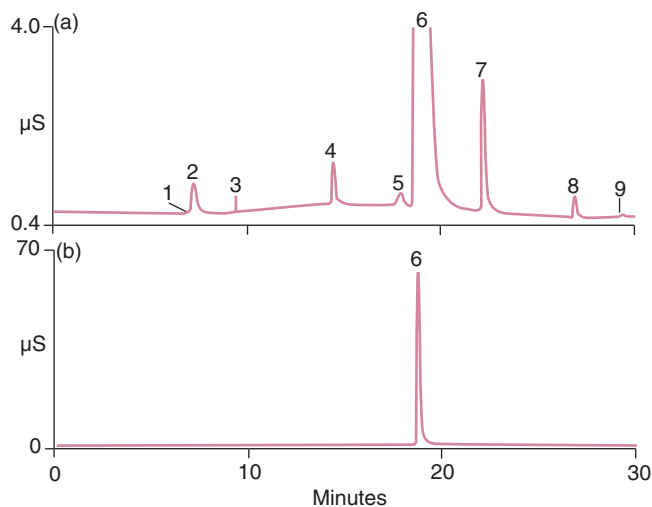


Figure 13.3. Separation of sulfate counterion and anionic impurities in Humatin®. Column: IonPac AS11-HC (2 × 250 mm); eluent: 1 mM KOH from 0–5 min, then 1–5 mM 5–9 min, 5–38 mM 9–20 min, 38–60 mM 20–25 min, 60 mM 25–30 min; eluent source: eluent generator cartridge; flow rate: 0.38 mL/min; column temperature: 30°C; detection: suppressed conductivity; injection volume: 5 µL; sample: (a) 2.5 mg/mL Humatin, (b) 0.25 mg/mL Humatin; analytes: (1) unknown, (2) 0.080% acetate, (3) unknown, (4) 0.025% chloride, (5) carbonate, (6) 24.7% sulfate, (7) 0.23% phosphate, (8) 0.0035% pyrophosphate, (9) unknown.

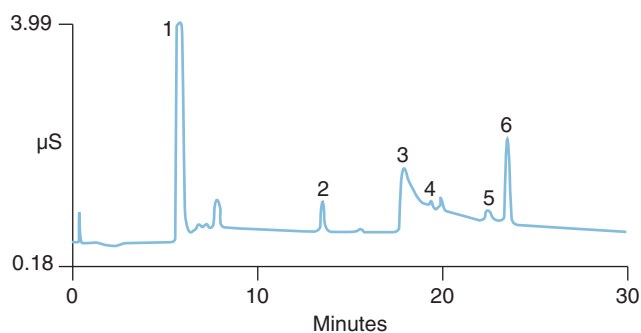


Figure 13.7. Separation of anionic impurities of a proprietary pharmaceutical compound, which has poor solubility in water. Column: IonPac AS15 (2 × 250 mm); eluent: 10 mM KOH 0–8 min, then 10–40 mM KOH 8–14 min, 40–60 mM KOH 14–20 min, 60 mM KOH 20–30 min; eluent source: eluent generator cartridge; flow rate: 0.40 mL/min; column temperature: 30°C; detection: suppressed conductivity; injection volume: 100 µL; matrix elimination volume: 1 mL (deionized water); sample: 0.30 mg/mL pharmaceutical compound in 100% methanol; analytes: (1) 975 µg/L fluoride, (2) 33.3 µg/L chloride, (3) carbonate, (4) 6.5 µg/L sulfate, (5) 33.8 µg/L nitrate, (6) 339 µg/L phosphate.

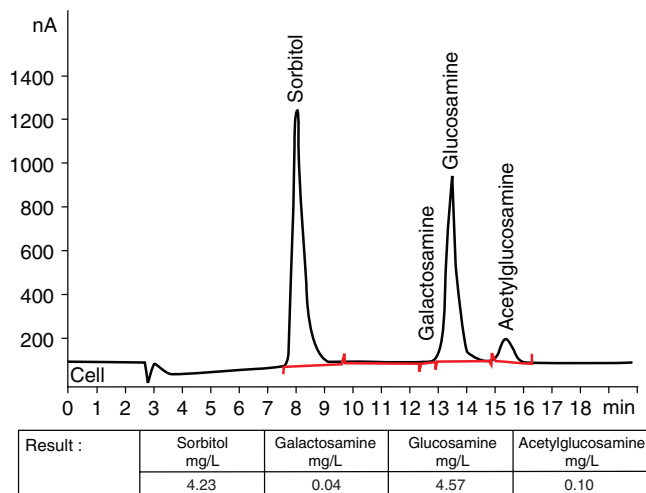


Figure 14.5. Example of pharmaceutical product analysis using in-line ultrafiltration. Electro Chemical Detector waveform used for detection: $E1 = +0.05V$, $E2 = +0.75V$, $E3 = -0.15V$, $t1 = 0.40s$, $t2 = 0.20s$, $t3 = 0.40 s$, sample time = 100ms, Detector Range = 0–5 μA full scale, 0% offset.

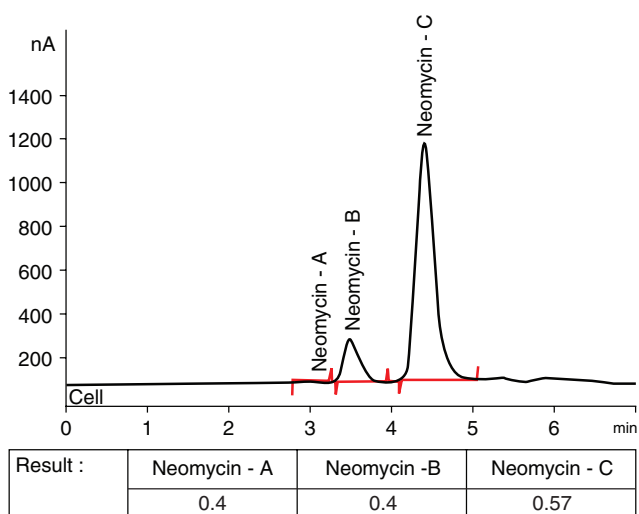
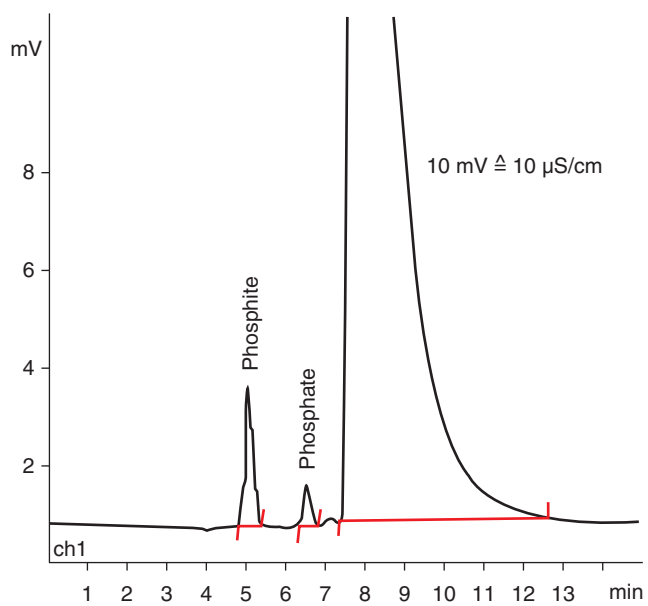


Figure 14.6. Example of neomycin powder analysis using in-line ultrafiltration. Electro Chemical Detector waveform used for detection: $E1 = +0.05 V$, $E2 = +0.75 V$, $E3 = -0.15 V$, $t1 = 0.40 s$, $t2 = 0.20 s$, $t3 = 0.40 s$, sample time = 100 ms, Detector Range = 0–5 μA full scale, 0% offset.



Result :	Phosphite wt %	Phosphate wt %
	0.029	0.775

Figure 14.8. Example of the Pamidronic Acid analysis using in-line dialysis (Column ASUPP3-4 mm ID x 250 mm length at 35°C).

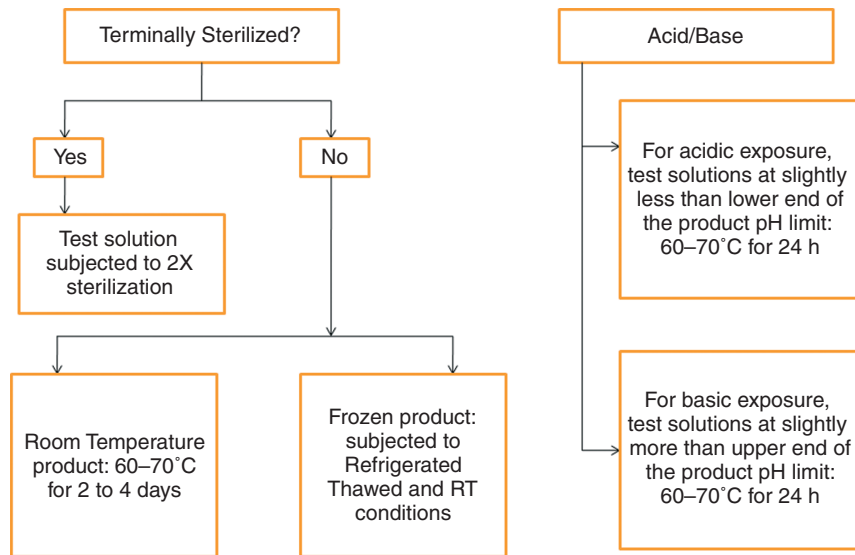


Figure 15.1. Recommended forced degradation scheme with respect to heat and acid/base for injectable drug products.

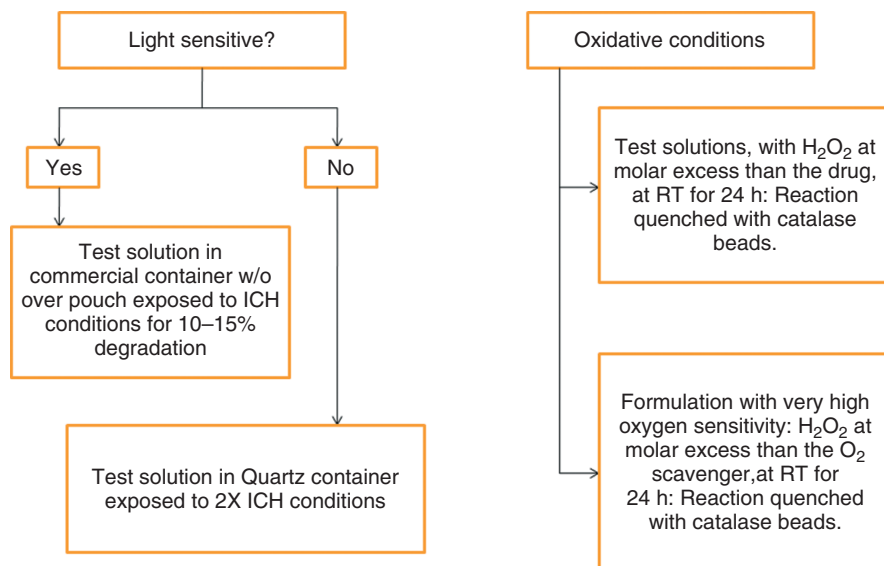


Figure 15.2. Recommended forced degradation scheme with respect to light and oxidative conditions for injectable drug products.

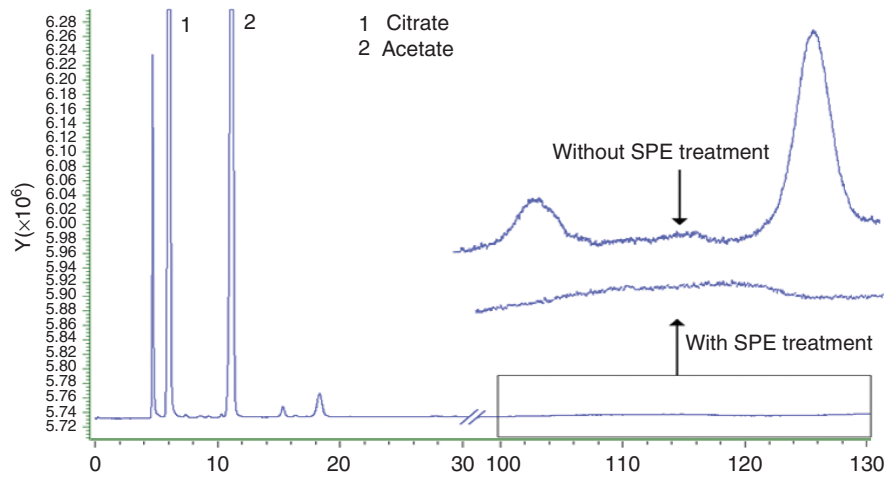


Figure 15.3. Chromatogram illustrating removal of late-eluting peaks in a medical fluid sample treated by SPE. An 8-mL sample was pushed through the SPE cartridge and discarded. Another 1 mL was then pushed through the cartridge and collected for the IEC analysis. Chromatographic conditions, Mobile phase; 50 mN H_2SO_4 0.8 mL/min, columns; 4.6 \times 30 mm cation H^+ guard cartridge and 7.8 \times 300 mm HPX-87H analytical column, 20 μL injection, 60 $^\circ$ C column temperature, and UV detection at 210 nm.

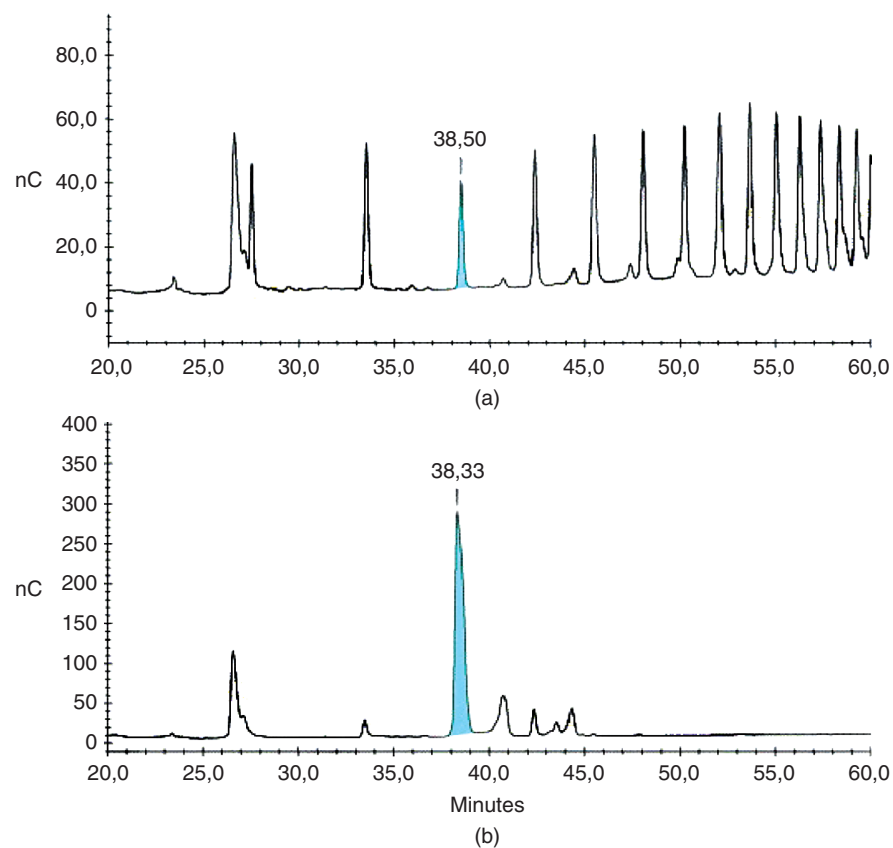


Figure 22.6. HPAEC-PAD profiling using a CarboPac PA100 column of: (a) oligosaccharides after acid hydrolysis of Men Y capsular PS (b) purified oligosaccharide of degree of polymerization (DP) = 4, Rt = 38 minutes. The numbers in the chromatograms indicate the retention times. DP4 peaks are highlighted. Reprinted from Ref. 32 with permission from Elsevier.

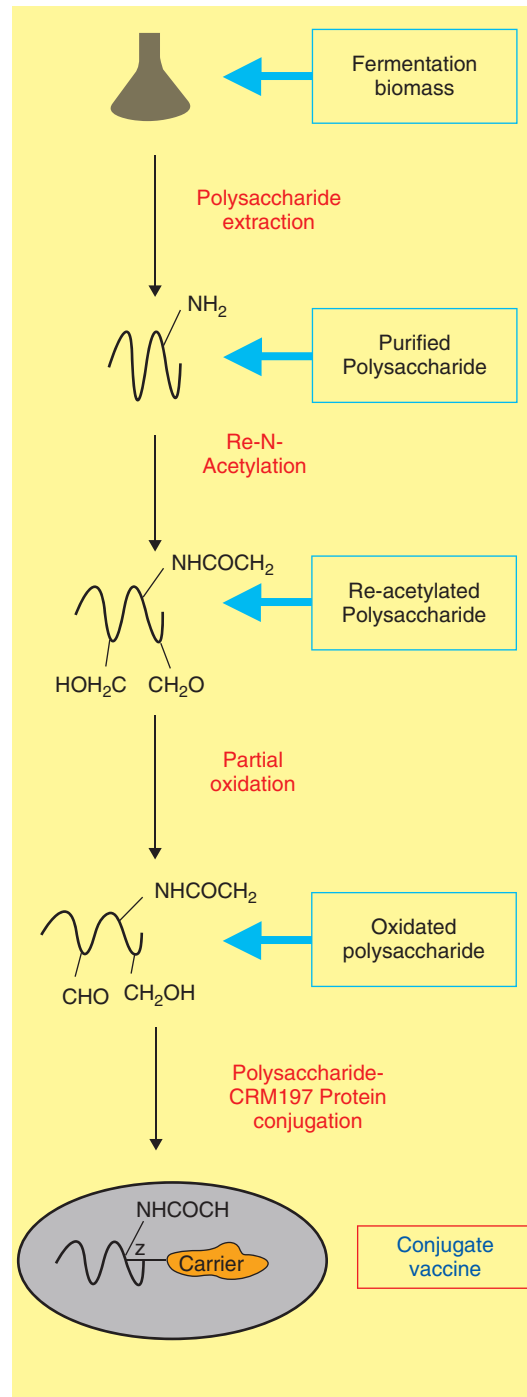


Figure 23.1. General scheme of glycoconjugate vaccine production.

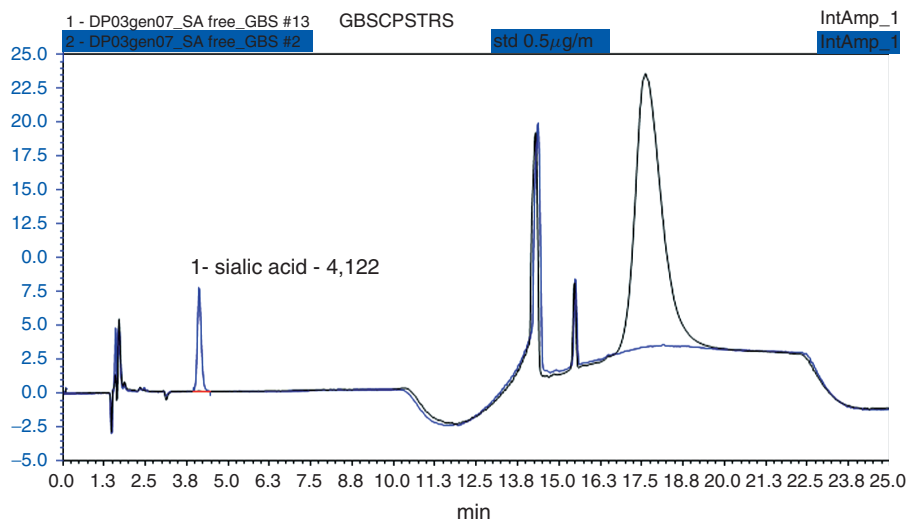


Figure 23.2. Overlay of standard sialic acid injection (blue chromatogram) and sample injection (black chromatogram). The sample does not contain any free sialic acid and the large peak in the regeneration step is the whole polysaccharide.

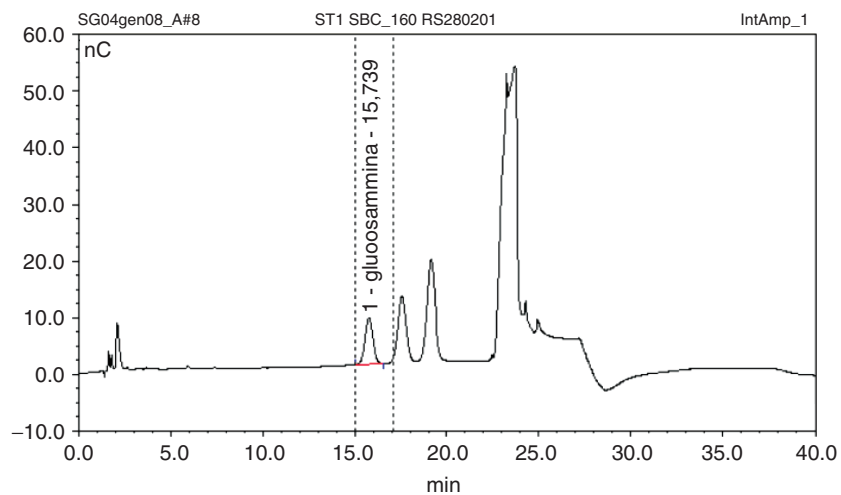


Figure 23.3. Sample of GBS polysaccharide serotype V hydrolyzed. The glucosamine peak is labeled.

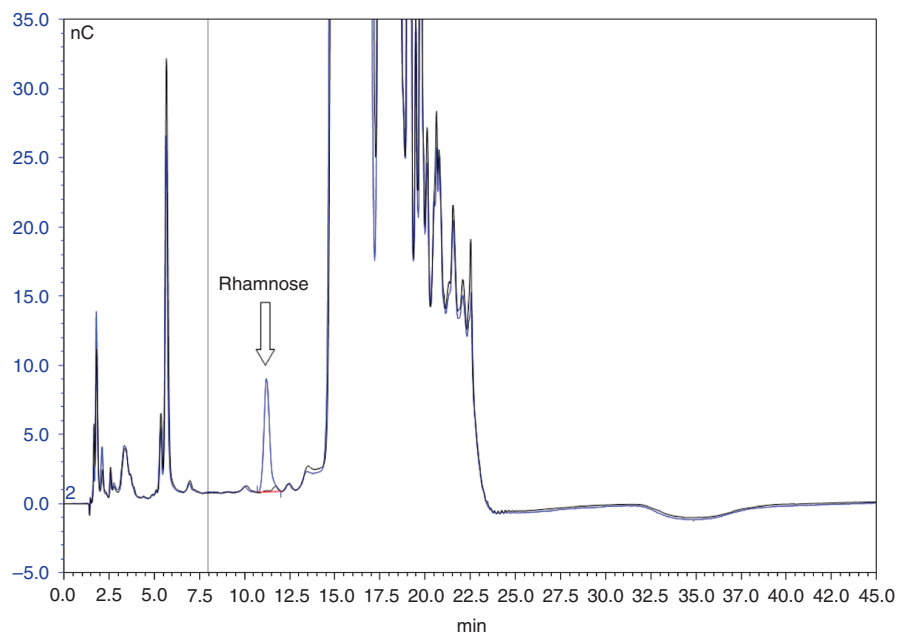


Figure 23.5. The sample is a purified GBS polysaccharide treated as described. The sample does not present a rhamnose peak. The blue chromatogram is obtained by adding rhamnose standard to the sample.

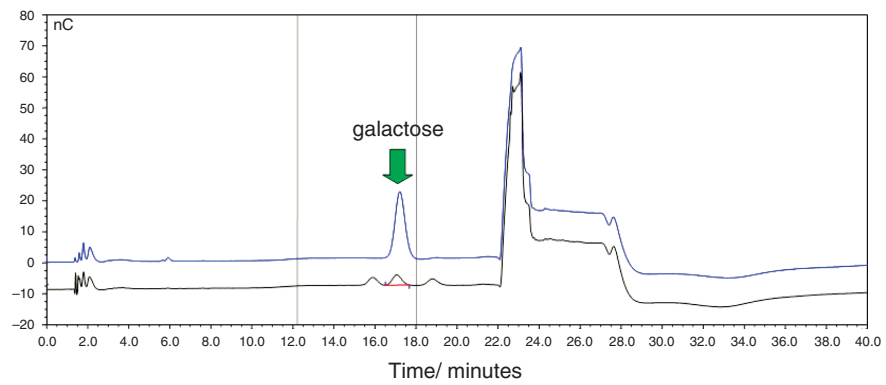
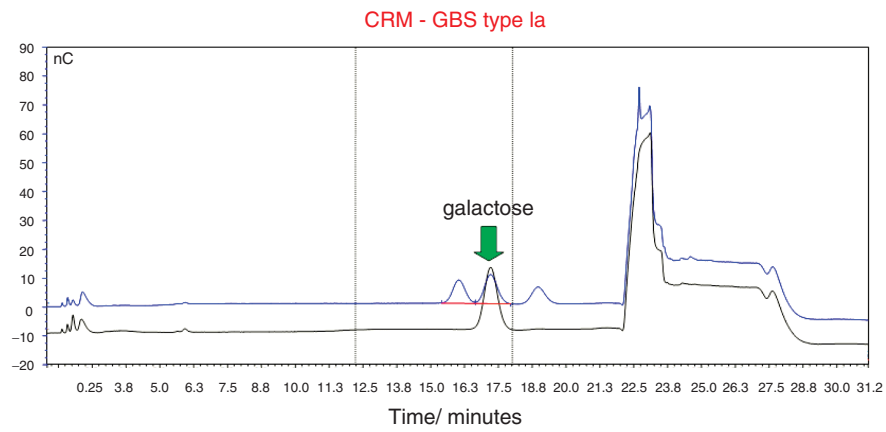


Figure 23.6. Galactose determination in concentrate bulk serotype Ia. Total and free saccharide chromatograms are reported. An overlay with galactose standard is reported in order to identify the galactose peak in the sample.

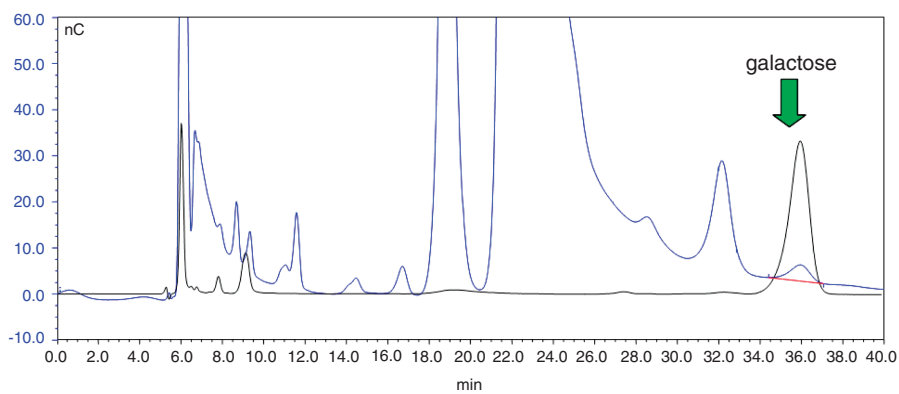
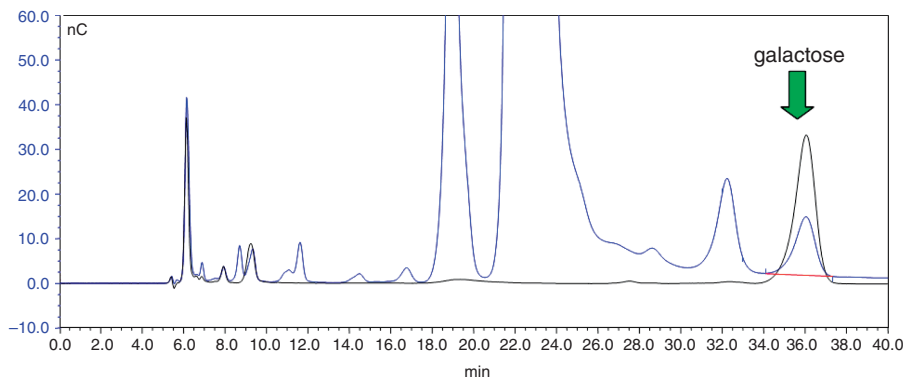


Figure 23.7. Determination of galactose in lyophilized CRM-GBS serotype Ia glycoconjugate by CarboPac MA1 chromatography. In each figure the black chromatogram is the galactose standard and the blue chromatogram is the sample. The upper panel is total saccharide determination and the lower panel is the free saccharide determination.

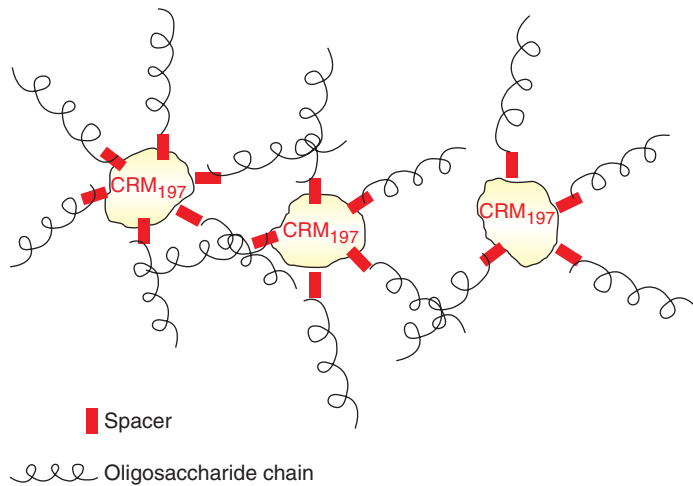


Figure 24.1. Schematic structure of glycoconjugate molecules: oligosaccharide chains covalently attached to a non-toxic mutant of the diphtheria toxoid CRM₁₉₇.

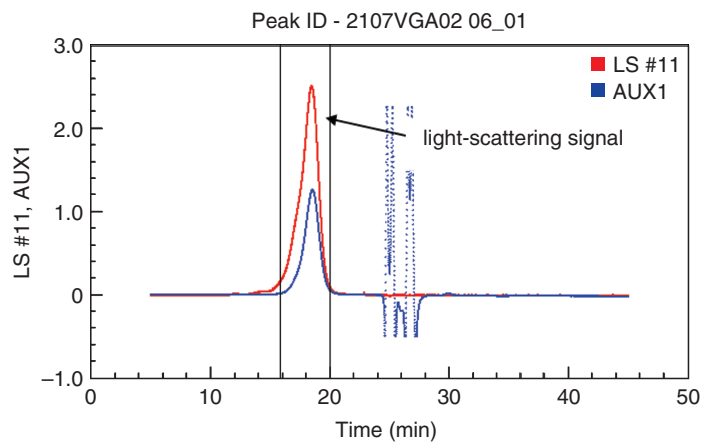


Figure 24.2. Typical SEC/MALLS elution profiles from light-scattering and RI detectors for MenA-CRM₁₉₇. The vertical bars indicate the integration limits for the peak. Samples were eluted at a flow rate of 0.8 mL/min in 0.2M sodium phosphate buffer pH 7.0 on tandem Ultrahydrogel™ 1000 and 250 columns.

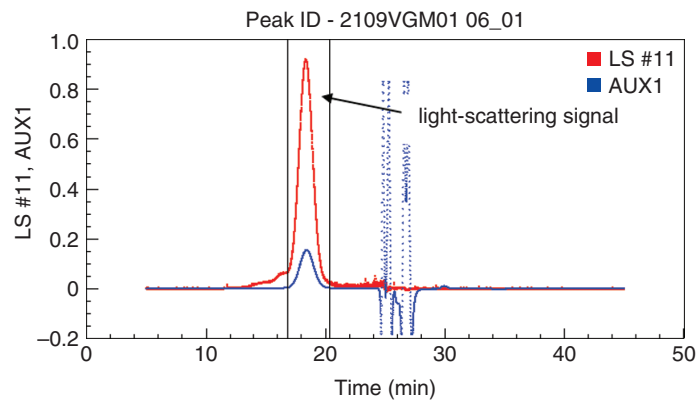


Figure 24.3. Typical SEC/MALLS elution profiles from light-scattering and RI detectors for MenC-CRM₁₉₇. The vertical bars indicate the integration limits for the peak. Conditions were the same as Figure 24.2.

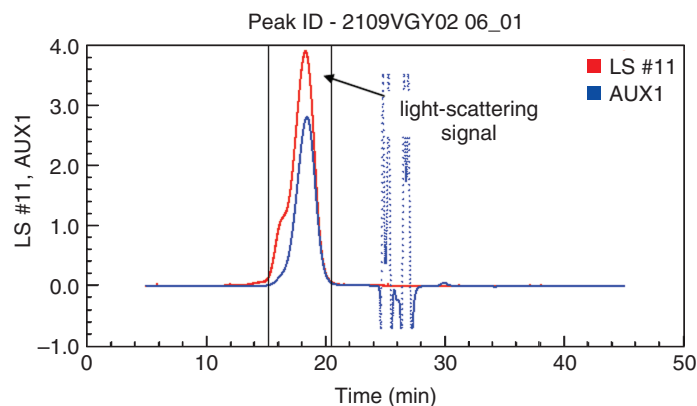


Figure 24.4. Typical SEC/MALLS elution profiles from light-scattering and RI detectors for MenY-CRM₁₉₇. The vertical bars indicate the integration limits for the peak. Conditions were the same as Figure 24.2.

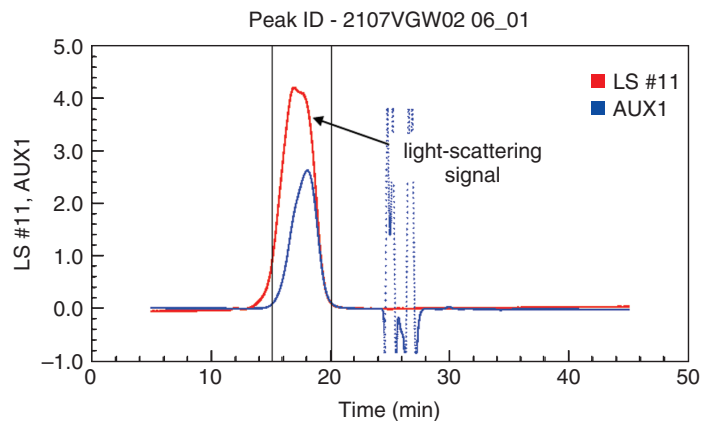


Figure 24.5. Typical SEC/MALLS elution profiles from light-scattering and RI detectors for MenW-CRM₁₉₇. The vertical bars indicate the integration limits for the peak. Conditions were the same as Figure 24.2.

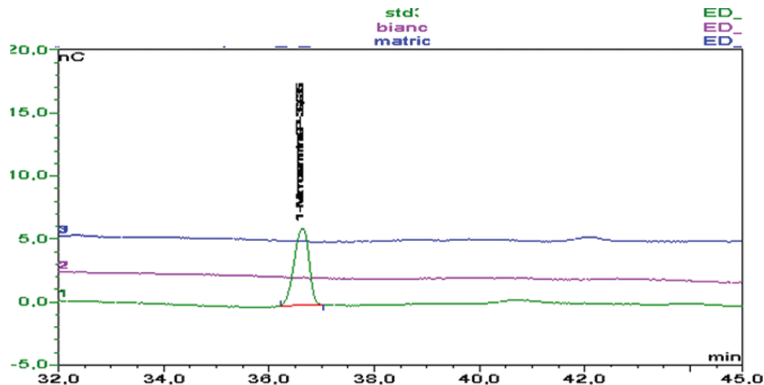


Figure 24.6. HPAEC-PAD chromatograms of blank, matrix, and standard on CarboPac PA10 column in the Specificity Test. The chromatographic analyses were performed with a flow rate of 1.0 mL/min and a run time of 55 min by a gradient mode using 100 mM NaOH and 1M sodium acetate/100 mM NaOH. The peak is the mannosamine-6-P standard (2.0 µg/mL).

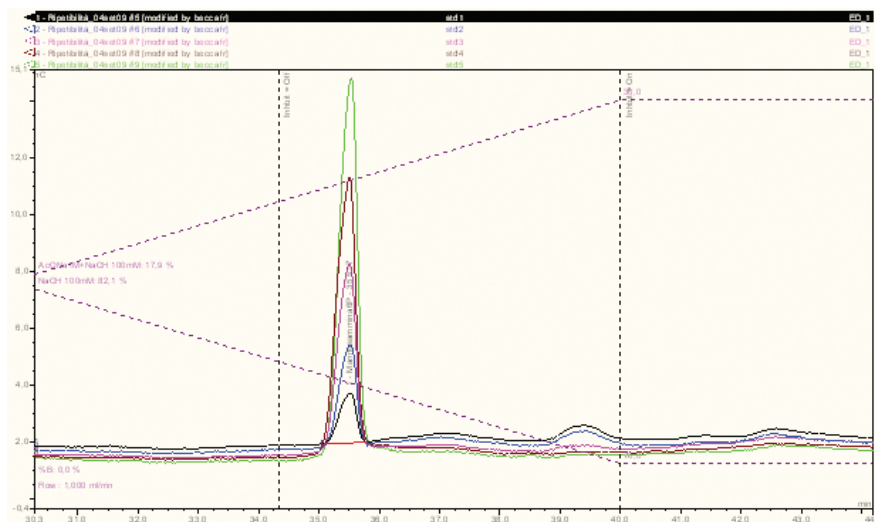


Figure 24.7. Overlay of HPAEC-PAD chromatograms of ManN6P standard points. The amount of total MenA saccharide is extrapolated using a calibration standard curve constituted of 5 Man-6-P standard points (1.0 $\mu\text{g/mL}$ –2.0 $\mu\text{g/mL}$ –4.0 $\mu\text{g/mL}$ –6.0 $\mu\text{g/mL}$ –8.0 $\mu\text{g/mL}$). The linearity is good over the range of concentrations tested with correlation coefficient greater than 0.99.

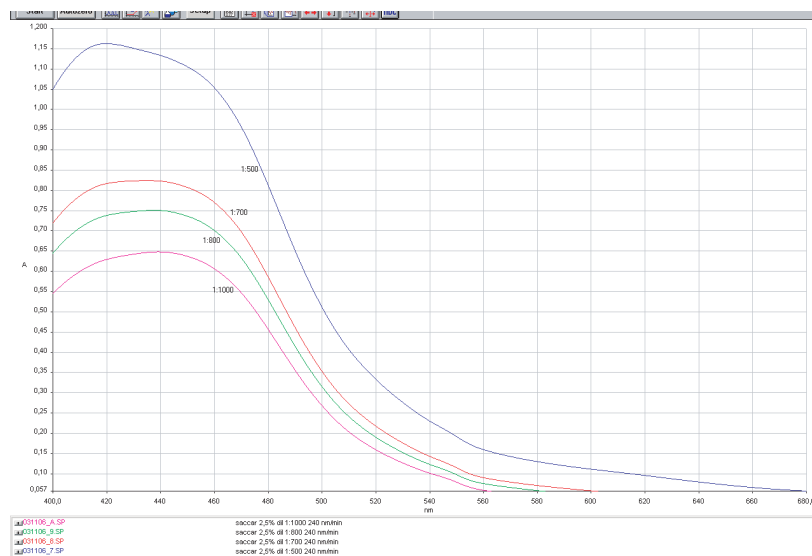


Figure 24.8. Overlay of spectra of sucrose solutions at different concentrations. Spectra of aqueous solutions of sucrose at different concentrations have shown the high absorption and therefore interference of sucrose to wavelength of 564 nm.

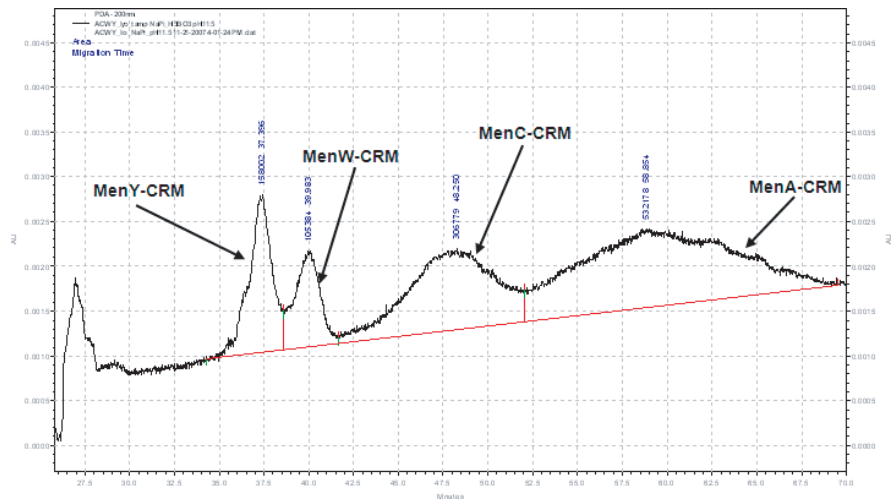


Figure 24.9. CZE analysis of MenACYW vaccine: UV detection 200 nm. It is possible to identify the single glycoconjugates that comprise the MenACYW vaccine by capillary electrophoresis analysis. No sample pre-treatments were performed on the sample before injection in the CE system.

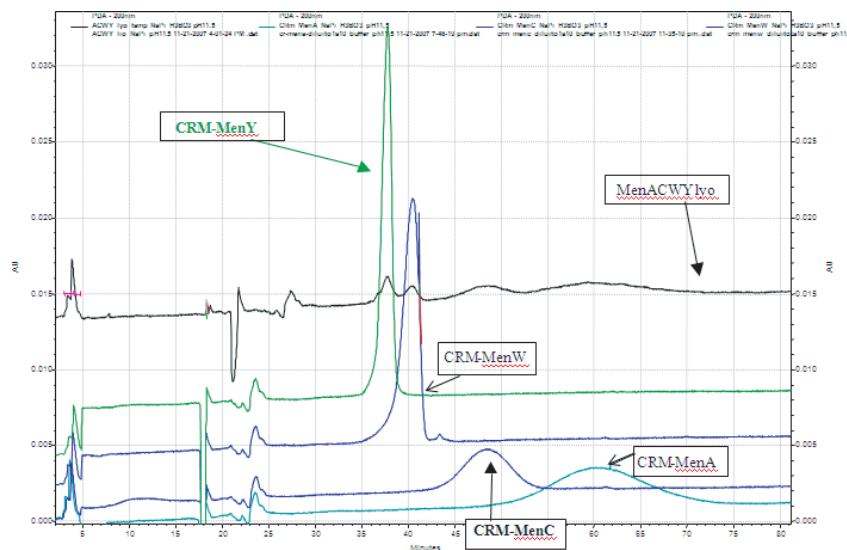


Figure 24.10. Overlay of electrophoregrams obtained from MenACYW vaccine and single concentrated bulks. The single glycoconjugates show the same migration time in the MenACYW formulation.